

1 **Manuscript title:**

2 In utero exposure to per – and polyfluoroalkyl substances (PFAS) associates with altered human
3 infant T helper cell development.

4 **Authors:**

5 Darline Castro Meléndez, Department of Immunology, Microbiology and Virology, University of
6 Rochester School of Medicine and Dentistry, Rochester, NY, USA.

7 Nathan Laniewski, Department of Pediatrics, University of Rochester School of Medicine and
8 Dentistry, Rochester, NY, USA.

9 Todd A. Jusko, Department of Public Health Sciences, University of Rochester School of Medicine
10 and Dentistry, Rochester, NY, USA.

11 Xing Qiu, Departments of Biostatistics and Computational Biology, University of Rochester School
12 of Medicine and Dentistry, Rochester, NY, USA.

13 B. Paige Lawrence, Department of Environmental Medicine, University of Rochester School of
14 Medicine and Dentistry, Rochester, NY, USA.

15 Zorimar Rivera-Núñez, Department of Biostatistics and Epidemiology, Rutgers School of Public
16 Health, Environmental and Occupational Health Sciences Institute; Piscataway, New Jersey, USA.

17 Jessica Brunner, Department of Obstetrics and Gynecology, University of Rochester School of
18 Medicine and Dentistry, Rochester, NY, USA.

19 Meghan Best, Department of Obstetrics and Gynecology, University of Rochester School of
20 Medicine and Dentistry, Rochester, NY, USA.

21 Allison Macomber, Department of Obstetrics and Gynecology, University of Rochester School of
22 Medicine and Dentistry, Rochester, NY, USA.

23 Alena Leger, Department of Obstetrics and Gynecology, University of Rochester School of Medicine
24 and Dentistry, Rochester, NY, USA.

25 Kurunthachalam Kannan, Department of Environmental Health Sciences, College of Integrated
26 Health Sciences, University at Albany, Albany, NY, USA and Wadsworth Center, New York State
27 Department of Health, Albany, NY, USA

28 Richard Kermit Miller, Department of Obstetrics and Gynecology, University of Rochester School of
29 Medicine and Dentistry, Rochester, NY, USA.

30 Emily S. Barrett, Department of Biostatistics and Epidemiology, Rutgers School of Public Health,
31 Environmental and Occupational Health Sciences Institute; Piscataway, New Jersey, USA.

32 Thomas G. O'Connor, Departments of Psychiatry, Neuroscience, Obstetrics and Gynecology,
33 University of Rochester School of Medicine and Dentistry, Rochester, NY, USA.

34 Kristin Scheible, Department of Pediatrics, University of Rochester School of Medicine and
35 Dentistry, Rochester, NY, USA.

36 **Contact Information corresponding author:**

37 Kristin Scheible, MD

38 Kristin_Scheible@URMC.Rochester.edu

39 University of Rochester

40 601 Elmwood Avenue, Box 651

41 Rochester, NY 14642

42

43 **Declaration of competing financial interests (CFI):**

44 The authors declare they have no actual or potential competing financial interests.

45

46

47

48

49

50

51

52

53

54

55

56

57

58 **Abstract:**

59 **Background:**

60 Environmental exposures to chemical toxicants during gestation and infancy can dysregulate
61 multiple developmental processes, causing lifelong effects. There is compelling evidence of PFAS-
62 associated immunotoxicity in adults and children. However, the effect of developmental PFAS
63 exposure on infant T-cell immunity is unreported, and, if present, could be implicated in immune-
64 related health outcomes.

65 **Objectives:**

66 We seek to model longitudinal changes in CD4+ T-cell subpopulations from birth through 12
67 months and their association with in-utero PFAS exposure and postnatal CD4+ T-cell frequencies
68 and functions.

69 **Methods:**

70 Maternal-infant dyads were recruited as part of the UPSIDE-ECHO cohort during the first trimester
71 between 2015 and 2019 in Rochester, New York; dyads were followed through the infant's first
72 birthday. Maternal PFAS concentrations (PFOS, PFOA, PFNA, and PFHXS) were quantified in serum
73 during the second trimester using high-performance liquid chromatography and tandem mass
74 spectrometry. Infant lymphocyte frequencies were assessed at birth, 6- and 12-months using mass
75 cytometry and high-dimensional clustering methods. Linear mixed-effects models were employed
76 to analyze the relationship between maternal PFAS concentrations and CD4+ T-cell subpopulations
77 (n=200). All models included a PFAS and age interaction and were adjusted for parity, infant sex,
78 and pre-pregnancy body mass index.

79 **Results:**

80 In-utero PFAS exposure correlated with multiple CD4+ T-cell subpopulations in infants. The greatest
81 effect sizes were seen in T-follicular helper (Tfh) and T-helper 2 (Th2) cells at 12 months. A log₂-unit
82 increase in PFOS was associated with lower Tfh [0.17% (95%CI: -0.30, -0.40)] and greater Th2
83 [0.27% (95%CI: 0.18, 0.35)] cell percentages at 12 months. Similar trends were observed for PFOA,
84 PFNA, and PFHXS.

85 **Discussion:**

86 Maternal PFAS exposures correlate with cell-specific changes in the infant T-cell compartment,
87 including key CD4+ T-cell subpopulations that play central roles in coordinating well-regulated,
88 protective immunity. Future studies into the role of PFAS-associated T-cell distribution and risk of
89 adverse immune-related health outcomes in children are warranted.

90 Introduction

91 The immune system development begins in the fetus during gestation and continues after birth.
92 Different immune cell types arise from precursors, which can differentiate and develop in a
93 regulated manner.¹⁻³ Environmental exposure to harmful agents such as chemical toxicants or
94 deficits in nutrition during gestation and infancy can dysregulate multiple developmental processes
95 influencing health over a lifetime.⁴⁻⁷ Among these harmful agents, exposure to per- and
96 polyfluoroalkyl substances (PFAS) stands out due to their widespread prevalence and persistence
97 in the environment,⁸ and their well-documented associations with several adverse health
98 outcomes across the lifespan, including impaired reproduction, growth, neurodevelopment and
99 liver, kidney and immune dysfunction.⁹⁻¹⁴ PFAS are a group of synthetic chemicals characterized by
100 interconnected carbon and fluorine (C-F) atom chains.⁸ The strong C-F bond makes PFAS
101 resistant to environmental and physiological breakdown processes and allows them to accumulate
102 and persist in the environment and human tissues.¹⁵ In the U.S., over 97% of the population has
103 detectable concentrations of PFAS in their blood¹⁶, and similar findings have been reported in
104 studies from Spain,¹⁷ Germany,¹⁸ and China.¹⁹ In addition to blood, PFAS have been detected in
105 human lungs, brain, bone, liver, and kidneys.¹⁵ PFAS have also been detected in the placenta, cord
106 blood, and breast milk,²⁰⁻²⁵ which further emphasizes the potential for early life exposures.

107 One consistent observation is an inverse association between PFAS concentrations and antibody
108 responses to vaccinations in adults and children.^{9,10,26-30} It is unclear which immune system
109 components are affected by PFAS to generate a net effect of lower humoral responses. The
110 production of antibodies results from the collaboration between multiple types of immune cells.³¹
111 When the immune system is stimulated by vaccinations or infections, cells from the innate
112 compartment, such as macrophages and neutrophils, trigger inflammatory processes that activate
113 cells of the adaptive immune system (T and B-cells), which can then establish immune memory.
114 Immune memory is the ability of cells to retain antigen-specific information from prior exposures to
115 facilitate a faster and more targeted response upon subsequent encounters. Antibody production
116 by B-cells is influenced by CD4+ T-cells, which consist of different specialized subpopulations
117 tailored to the immune response needed for a specific pathogen or antigen.³² These include Th1,
118 Th2, Th17, T follicular helper cells (Tfh), and T regulatory cells (Treg).³³ Each CD4+ T-cell subset
119 carries a unique set of functions that influence B-cells by modulating the strength, specificity, and
120 durability of their produced antibodies.³⁴ For example, long-lived B-cells rely on Tfh cells for

121 durable antibody production because Tfh cells promote germinal center formation in lymph nodes
122 via IL-21 secretion.³⁵⁻⁴⁰ This interaction leads to B-cell proliferation, somatic hypermutation, and
123 isotype class switching, ultimately resulting in high-affinity antibodies.^{35,37} Other CD4+ T-cell
124 subpopulations modulate antibody class switching by fine-tuning the context of the immune
125 response required.⁴¹⁻⁴⁴ How early life exposures to PFAS affects these cell types is crucial for
126 discovering how PFAS ultimately leads to changes in immune responses. This longitudinal study
127 aims to identify alterations in CD4+ T-cells related to developmental PFAS exposure as a first step
128 in understanding pathways implicated in PFAS-related immune dysfunction.

129 **Methods:**

130 ***Study design***

131 Between December 2015 and April 2019, first-trimester pregnant women were recruited from
132 outpatient clinics affiliated with the University of Rochester and enrolled in the Understanding
133 Pregnancy Signals and Infant Development and Environmental Influences on Child Health
134 Outcomes (UPSIDE-ECHO) study after informed consent. UPSIDE-ECHO is an ongoing prospective
135 birth cohort designed to study prenatal exposures in relation to perinatal and child health
136 outcomes in the Rochester, NY, area⁴⁵ that is part of the NIH ECHO program.⁴⁶ Eligibility criteria
137 included maternal age 18 years or older, singleton pregnancy, no known substance abuse problems
138 or history of psychotic illness, and the ability to communicate in English. Participants with major
139 endocrine disorders (e.g., polycystic ovary syndrome) and high-risk pregnancies at baseline were
140 not enrolled; additionally, infants born prior to 37 weeks of gestation or with congenital anomalies
141 or significant health problems were excluded (n=9). Study visits, including physical exams,
142 biospecimen collection, and questionnaire completion, were completed at each trimester and at
143 birth, 6 and 12 months postnatally. This study protocol was approved by the University of Rochester
144 School of Medicine and Dentistry Institutional Review Board (#58456).

145 ***Maternal and infant blood collection***

146 During the second trimester of pregnancy (21 ± SD:1.8) gestational weeks), maternal serum from
147 blood collected into EDTA tubes was frozen at -80°C until the time of analysis. For infant blood
148 samples, cord blood was collected by venipuncture into sodium heparin tubes immediately after
149 birth. Infant blood was collected into sodium heparin tubes at 6 and 12 months. Peripheral blood
150 mononuclear cells (PBMC) were isolated using a Ficoll-Paque density gradient (GE Healthcare –

151 cytiva) and immediately cryopreserved in freezing media consisting of 10% heat-inactivated Fetal
152 Bovine Serum (FBS)(Seradigm) and 10% DMSO (Amresco) at a cell concentration ranging from one
153 to five million cells per mL.

154 ***PFAS analysis***

155 Maternal serum isolated from the second trimester of pregnancy was sent to Wadsworth Center's
156 Human Health Exposure Analysis Resource (HHEAR) Laboratory Hub for PFAS measurement. PFAS
157 were measured using high-performance liquid chromatography (HPLC) and tandem mass
158 spectrometry (MS/MS) detection and quantification, as described in Honda et al. (2018).⁴⁷ Fourteen
159 PFAS were measured: NETFOSAA, NMFOSAA, PFBS, PFDA, PFDODA, PFHPA, PFHXA, PFHXS,
160 PFNA, PFOA, PFOS, PFOSA, PFPEA, PFUNDA. The limit of detection (LOD) for individual PFAS
161 varied from 0.02 to 0.03 ng/mL. To reduce exposure misclassification, four PFAS with 100%
162 detection rate, namely PFOA, PFOS, PFNA, and PFHXS were included in the present analysis.
163 Several quality control samples namely certificated standard reference materials (NIST SRM 1957
164 and SRM 1958), HHEAR QC pools, procedural blanks and matrix spikes were included in the
165 analysis. The coefficient of variation in concentrations of four PFAS in SRMs, QC pools and matrix
166 spikes between batches was <10%.

167 ***Infant T-cell phenotyping***

168 Thawing, stimulation, and staining of PBMCs for mass cytometry were performed as detailed
169 previously Scheible et al. (2012) and McDavid et al. (2022).^{48,49} To control for batch effect and
170 variability, all timepoints (birth, 6, and 12 months) from individual infant subjects were phenotyped
171 in experimental batches that included 20 individual samples maximum. Each experimental batch
172 also included one to two healthy adult PBMC controls that were carried across multiple batches.
173 Cryopreserved sample vials were thawed at 37°C in a water bath and washed twice with 10mL of
174 RPMI 1640 (Corning) supplemented with L-glutamine, 10% heat-inactivated Fetal Bovine Serum
175 (FBS) (R10), and 25U/uL Universal Nuclease (R10+n). Cord blood samples (CBMC) were treated
176 with 3 mL 1x BD Pharm Lyse (BD Biosciences) supplemented with 25U/uL Universal Nuclease for 15
177 minutes to lyse red blood cells. Washed cells were rested overnight at 37°C in a 5% CO₂ incubator.
178 After overnight rest, samples were counted on a dual-fluorescence cell counter (Cellometer K2;
179 Nexcelom/Revvity); samples less than 70% viable were excluded from the assay (5.9% of samples
180 at birth, 14.6% at 6 months and 12.7% at 12 months). Cells were resuspended in R10 at a

181 concentration of 30 million-cells/mL, and 3 million cells were stimulated for 2 hours with 2ug/mL of
182 *Staphylococcus aureus*, Enterotoxin Type B (SEB). GolgiPlug (BD Biosciences) and monensin
183 (Sigma; 10 mM stock in EtOH) were added at 2 hours and further stimulated for 8 hours at 37°C.
184 Stimulated cells were washed with stain buffer (PBS + 2%FBS + 25U/uL Universal Nuclease) (SBn)
185 and stained for 30 minutes at room temperature (RT) with unique combinations of metal-
186 conjugated anti-human CD45 antibodies (Supplemental Table 1: Parameter Type, Barcodes) in a ‘6-
187 choose-3’ or ‘7-choose-3’ live-cell barcoding scheme.^{50–52} Barcoded samples were washed,
188 resuspended in SBn, and then transferred into a single 15mL culture tube. The pooled sample was
189 filtered, centrifuged, and stained for 30 minutes at RT with a cocktail of metal-conjugated anti-
190 human antibodies for surface molecules (Supplemental Table 1: Parameter Type, Surface). Next,
191 cells were washed with SBn then stained with Cell-ID Cisplatin-194Pt (Fluidigm/Standard BioTools)
192 at 500nM/mL concentration for 5 minutes at RT. Cells were washed with SBn and
193 fixed/permeabilized for 30 minutes at RT with Foxp3 Fixation-Permeabilization buffer (eBioscience)
194 followed by a wash with Permeabilization Buffer (Perm-B) (eBioscience). Cells were intracellularly
195 stained for 30 minutes at RT with Perm-B containing a cocktail of metal-conjugated anti-human
196 antibodies (Supplemental Table 1: Parameter Type, Intracellular). Cells were washed, then fixed
197 with 1 mL of 1.6% formaldehyde (Pierce) in PBS containing 500 nM of Cell-ID Intercalator-103Rh
198 (Fluidigm/Standard BioTools) and incubated overnight at 4°C. Fixed cells were washed with PBS,
199 counted, and resuspended at a concentration of 13.75 million-cells/mL in filtered FBS with 10%
200 DMSO (Amresco). Cells were aliquoted in Protein Lo-Bind tubes (Eppendorf) (2.75 million cells in
201 200ul) and stored at -80°C. Following aliquoting and freezing, individual aliquots were prepared for
202 acquisition on a CyTOF 2 or Helios mass cytometer (Fluidigm/Standard BioTools) by washing twice
203 with 2 mL ultrapure water and resuspending in 3 mL ultrapure water containing 0.1x EQ Four
204 Element Calibration Beads (Fluidigm/Standard BioTools). Aliquots were acquired using a Super
205 Sampler (Victorian Airships).

206 *Mass cytometry clustering pipeline*

207 After the acquisition, source data was normalized using the Normalization Passport in CyTOF
208 Software with default settings (Fluidigm, 7.0.5189). Normalized data was analyzed using a custom
209 R-based workflow (github.com/nlaniewski/SOMnambulate). Briefly, unique live-cell barcoded pools
210 were debarcoded to generate sample-specific .fcs files. FlowSOM⁵³ was used to generate clusters
211 representing major PBMC immune cell populations (Supplemental Table 1: FlowSOM dimension,

212 PBMC). Based on per-cluster feature expression, annotations were defined. Selecting for only
213 CD3+, CD4+, and CD8+ clusters representing T-cells, a second FlowSOM was generated using an
214 expanded set of both surface and intracellular markers to define T-cell-specific sub-clustering
215 results (Supplemental Table 1: FlowSOM dimension, T-cells). As with the PBMC clusters, per-
216 cluster feature expressions were examined to define functional annotations. To aid in the
217 interpretation of FlowSOM clusters, the nodes that comprise the self-organizing map (SOM) were
218 visualized using Uniform Manifold Approximation and Projection (UMAP).⁵⁴ Default parameters
219 were used to embed the nodes into two dimensions, using the same markers as those used to
220 generate the respective SOM. Nodes (circles) were individually sized to represent the mean
221 proportion of assigned cells and colored by their assigned cluster annotation. For each FlowSOM
222 result (PBMC; T-cell), all cells were mapped on a per-sample basis, and the proportion of cells
223 attributed to each cluster was calculated. The proportions used in subsequent visualizations and
224 statistical models represent the percent of CD4+ T cells.

225 ***Measurement of covariates and selection of potential confounding variables.***

226 After study enrollment in the first trimester, trained staff administered a questionnaire to obtain
227 information on lifestyle, living environment, past pregnancies, medical conditions, medications
228 used before, during, and after pregnancy, and sociodemographic information. Sociodemographic
229 information, including self-reported maternal race and ethnicity, was collected at baseline,
230 recognizing that these social constructs are associated with environmental exposures and
231 maternal and child health outcomes.^{55,56} Infant birth weight and sex at birth were obtained from
232 electronic health records. Confounding variables were selected using a directed acyclic graph
233 (DAG) informed by previous reports demonstrating an association with PFAS and T-cells
234 (Supplemental Figure 1).^{10,57} These were the categorical variables parity, infant sex, mode of
235 delivery, maternal race, maternal education, and Medicaid during pregnancy, and the continuous
236 variables maternal age, pre-pregnancy body mass index (BMI), annual income, and infant birth
237 weight. The minimally sufficient set of variables from the DAG were categorical parity (0, 1, or 2+),
238 infant sex at birth, and continuous pre-pregnancy BMI.

239 ***Statistical analysis***

240 Descriptive characteristics for the entire sample are presented in Table 1. Specifically, frequencies
241 and percentages for categorical variables, as well as means with standard deviations for

242 continuous variables are reported in this table. Wilcoxon rank-sum test was used for comparing
243 mean differences between two groups for a continuous variable, Wilcoxon signed-rank test was
244 used to assess mean differences between two time points. The association between two
245 continuous variables was evaluated using Spearman's rank correlation test.

246 Owing to the longitudinal assessment of T-cell outcomes at multiple visits, two separate but
247 related Linear Mixed-Effect regression (LMER) modeling strategies were employed to associate T-
248 cell outcomes with individual PFAS concentrations, infant age, and their interactions. In both
249 models, infant age is considered as a categorical variable with three levels (birth, 6 and 12 months),
250 of which birth is considered as the baseline. In the first set of LMER models, a log-transformation
251 designed to reduce the skewness is applied to the PFAS concentration levels: $x_{ij} =$
252 $\log_2(\text{Conc}_{ij} + 1)$, where Conc_{ij} represents the original PFAS concentration level for the i th subject
253 at the j th visit. In the second set of LMER models, PFAS concentration levels were dichotomized as
254 “above median” or “below median”, permitting the estimation of differences in T-cell outcomes
255 over time as discrete categories according to the categorical interactions between infant age and
256 binary PFAS concentration levels. We call the second set of models as differences-over-time
257 models.

258 For both approaches, a model is called a *crude model* if it only includes a PFAS level, infant age,
259 and their interactions. It is called an *adjusted model*, if it also includes the following additional fixed
260 effects: parity (0, 1, or 2+), infant sex, and pre-pregnancy BMI (continuous). A subject-specific
261 random intercept was included in all models to account for serial correlation in the repeated T-cell
262 measures. Unknown parameters in these models were estimated by the Restricted maximum
263 likelihood (REML) criterion. Regression t-test implemented in R package *lmerTest*⁵⁸ was used to
264 assess the statistical significance of a fixed effect of interest; *F*-tests as implemented in function
265 *linearHypothesis()* in R package *car*⁵⁹ was used to test specific linear contrasts between infant
266 ages. Results for the difference-over-time models were presented as differences in marginal mean
267 percent with corresponding 95% confidence intervals, and pairwise comparisons were performed
268 to contrast mean percentages between below and above median PFAS. Model assumptions,
269 including normality, linearity, and homoscedasticity of the residuals, were visually evaluated by
270 inspection of diagnostic plots. A p-value of less than 0.05 was considered statistically significant
271 for individual hypothesis tests. For analyses involving multiple hypotheses, the Benjamini–

272 Hochberg procedure was employed to control the false discovery rate (FDR) at a level of 0.05. All
273 statistical analyses were conducted using R Foundation for Statistical Computing version 4.3.3.⁶⁰

274 **Results:**

275 ***Study Population***

276 The analysis included 200 full-term infants (Supplemental Figure 2). Participants were selected
277 from the larger UPSIDE-ECHO cohort if they had second-trimester maternal PFAS measured and
278 infant T-cell phenotyping from at least one timepoint (birth, 6, or 12 months of age). Cohort
279 characteristics are shown in Table 1. In summary, 71% of participants were between 26-35 years
280 old at enrollment; 62.5% of the cohort self-identified as White, 20% as Asian, 8% as Black, 9% as
281 Hispanic, and 10% as other. 52% reported having at least a bachelor's degree, and 43% were
282 enrolled in Medicaid during pregnancy. Parity was categorized based on pregnancies preceding the
283 current pregnancy (34.5% nulliparous, 39% primiparous, or 26.5% multiparous). The mean
284 gestational age at birth was $39.74 \pm \text{SD}:1.11$ weeks, 76.5% of infants were born vaginally, and 52.5%
285 were assigned male sex at birth. Among the 200 mother-infant pairs who contributed at least one
286 observation to the current study, compared to birth, those with 6- or 12-month data tended to be
287 older at the time of the child's birth, higher income and education, and more likely to report White
288 race (Supplemental Table 2).

289 ***PFAS exposure***

290 Table 2 shows the mean concentration and distribution of four PFAS (PFOS, PFOA, PFNA, and
291 PFHXS) that were detected in 100% of the second-trimester maternal serum samples and,
292 therefore, included in subsequent analysis. The concentrations and distribution of the ten
293 additional PFAS measured are in Supplemental Table 3. PFOS was present at the highest mean
294 concentration (2.87 ± 2.13 ng/mL), followed by PFHXS (1.96 ± 0.92 ng/mL), PFOA (0.68 ± 0.51 ng/mL),
295 and the lowest concentration being PFNA (0.33 ± 0.36 ng/mL). Relative to the NHANES general
296 population concentrations, PFOS, PFOA, and PFNA mean concentrations were lower.⁶¹ PFOA and
297 PFNA were the most strongly correlated ($\text{Rho}=0.64$, $p\text{-value}= 0.0001$), followed by PFOS and PFNA
298 ($\text{Rho}=0.58$, $p\text{-value}= 0.0002$) and PFOS and PFOA ($\text{Rho} = 0.53$, $p\text{-value}= 0.0005$). PFHXS showed
299 a moderate correlation with PFOS ($\text{Rho}= 0.38$, $p\text{-value}= 0.021$) and PFOA ($\text{Rho}= 0.30$, $p\text{-value}$
300 $=0.049$); PFNA and PFHXS were the most weakly correlated ($\text{Rho}= 0.23$, $p\text{-value} = 0.113$).

301 Determinants of exposure for the UPSIDE-ECHO population can be found in Supplemental Table 4.
302 Overall, the concentrations of all PFAS were lower, with higher maternal parity. Maternal PFAS
303 concentrations in serum were lower when the fetal sex was female. Generally, mean PFAS
304 concentrations were higher in white mothers and mothers with higher income and education, and
305 mean PFAS concentrations were lower in older mothers and mothers with higher pre-pregnancy
306 BMI. Participants with Medicaid during pregnancy had lower concentrations of PFAS.

307 ***Infant T-cell clustering and phenotyping***

308 A 36-marker mass cytometry panel (Supplemental Table 1) was used to deeply immunophenotype
309 infant immune cell populations over the first year of life. FlowSOM clustering algorithm was used to
310 identify and group immune populations (Figure 1A). PBMC populations were identified as follows:
311 $\gamma\delta$ T-cells were identified as CD3+ TCR $\gamma\delta$ + cells, cytotoxic T-cells as CD3+ CD8+, helper T-cells as
312 CD3+ CD4+, B-cells as CD19+, NK cells as CD56+, and monocytes as CD14+ cells. UMAP
313 visualization of infant leukocytes revealed separation between the major immune populations,
314 including T-cells, B-cells, NK cells, and monocytes (Figure 1B).

315 To test our specific hypothesis regarding the role of PFAS in T-cell development, we narrowed
316 analyses to CD4+ T-cells. CD4+ T-cells from the first level of clustering (i.e., PBMC) were then
317 selected for a second level of FlowSOM clustering using an expanded set of phenotypic and
318 functional markers to identify unique CD4+ T-cell sub-clusters. This sub-clustering analysis
319 identified 29 unique CD4+ T-cell sub-clusters (Supplemental Figure 3A-B). During the first year of
320 life, naïve (CD45RA+) comprised most of the CD4+ T-cell compartment, while T-cells carrying
321 markers of immunological memory (CD45RO+, CD45RA-) were a small fraction at birth and
322 increased over time (Figure 1C-D). Within the memory (CD45RO+) compartment, canonical CD4+
323 T-cell subpopulations Th1 (IFN γ +), Th2 (IL-4+), Th17 (IL-17A+), Tregs (FOXP3+ CD127-) and Tfh cells
324 (IL-21+) were identified based on the expression of surface and intracellular markers that
325 distinguish functional properties of these subpopulations (Figure 1E, Supplemental Figure 3B-C).
326 The percentages of these CD4+ T-cell subpopulations increased over time (Figure 1F, Supplemental
327 Table 5).

328 ***Maternal PFAS exposure associates with infant CD4+ T-cell frequencies in an age-dependent***
329 ***manner***

330 Figure 2 shows the age-specific adjusted association for PFOS, PFOA, PFNA, and PFHXS and each
331 CD4+ T-cell. The unadjusted and adjusted age-specific estimates for this model can be found in
332 Supplemental Table 6. Overall, the associations between PFAS and CD4+ T-cells were stronger at 6-
333 and 12-months of age versus birth; with statistical evidence of effect measure modification by age
334 for Tfh, Th2, and Th1 cells, but not for Tregs or Th17 cells (Supplemental Table 7 and Supplemental
335 Table 8). These associations were consistent for crude and adjusted models.

336 Tfh cells were inversely associated with maternal PFAS; each doubling of PFOS was associated with
337 a 0.17 (95%CI of β : -0.30, -0.04) lower Tfh percentage measured at 12 months of age, a 0.05 (95%CI
338 of β : -0.16, 0.06) lower Tfh percentage at 6 months, and a 0.08 (95%CI of β : -0.01, 0.16) greater Tfh
339 percentage at birth (p-value for age interaction=0.002). Similar trends were observed between Tfh
340 percentages and PFOA, PFNA and PFHXS (Figure 2A).

341 In contrast, Th2, Th1, and Treg cells were positively associated with maternal PFAS exposure. For
342 Th2 cells, each doubling of PFOA was associated with a 0.30 (95%CI of β : 0.18, 0.41) greater Th2
343 percentage measured at 12 months of age, a 0.25 (95%CI of β : 0.12, 0.38) greater Th2 percentage at
344 6 months, and a 0.05 (95%CI of β : -0.04, 0.14) greater Th2 percentage at birth (p-value for age
345 interaction = 0.000). Similar trends were observed between Th2 percentages and PFOS, PFNA, and
346 PFHXS (Figure 2B). For Th1 cells, each doubling of PFNA was associated with a 0.11 (95%CI of β :
347 0.02, 0.20) greater Th1 percentage measured at 12 months of age and no association at 6 months of
348 age or birth (p-value for age interaction = 0.054). Similar trends were observed between Th1
349 percentages and PFOS, PFOA, and PFHXS (Figure 2C).

350 For Tregs, each doubling of PFHXS was associated with a 0.11 (95%CI of β : 0.01, 0.22) greater Treg
351 percentage measured at 12 months of age, a 0.06 (95%CI of β : -0.02, 0.15) greater Treg percentage
352 at 6 months, and no association at birth (p-value for age interaction = 0.129). Similar trends were
353 observed between Treg percentages and PFOS, PFOA, and PFNA (Figure 2D). No associations were
354 observed between Th17 percentages and the doubling of PFOS, PFOA, PFNA, and PFHXS (Figure
355 2E).

356 ***Maternal PFAS exposure predicts CD4+ T-cell trajectories in infants.***

357 Overall, independently of PFAS exposure group, the trajectory of each CD4+ T-cell subset showed
358 increasing levels over time (Figure 3). Further, PFAS-dependent effects were more pronounced at
359 later ages, especially 12 months of age. This was the case for Tfh, Th2, Th1, and Treg cells, but not

360 for Th17 cells. Unadjusted and adjusted age-specific marginal means and pairwise comparisons
361 for below and above median PFAS can be found in Supplemental Tables 9 and 10, respectively. For
362 Tfh cells and PFOS exposure, the adjusted negative association was strongest at 12 months of age,
363 with a mean value for above median PFOS of $0.86 \pm \text{SD: } 0.05$ (95%CI:0.76, 0.96) versus a mean
364 value for below median PFOS of $1.13 \pm \text{SD: } 0.06$ (95%CI:1.02, 1.24) (p-value for difference=0.002);
365 similar trends were observed for PFOA and PFNA, and no differences were observed for PFHXS
366 (Figure 3A). For Th2 cells and PFOA exposure, the adjusted positive association was present at 6
367 months but stronger at 12 months of age. At 12 months we observed a mean value for Th2 cells for
368 above median PFOA of $0.44 \pm \text{SD: } 0.03$ (95%CI:0.37, 0.50) versus a mean value for below median
369 PFOA of $0.32 \pm \text{SD: } 0.04$ (95%CI: 0.25, 0.39) (p-value for difference = 0.002); similar trends were
370 observed for PFOS, PFNA, and PFHXS (Figure 3B). For Th1 cells and PFNA exposure, the adjusted
371 positive association was observed at 12 months of age, with a mean value for above the median
372 PFNA of $0.37 \pm \text{SD: } 0.02$ (95%CI: 0.32, 0.41) versus a mean value for below median PFNA of $0.30 \pm$
373 $\text{SD: } 0.02$ (95%CI: 0.25, 0.34) (p-value for difference = 0.019); similar trends were observed for PFOS,
374 PFOA, and PFHXS (Figure 3C). For Treg cells and PFHXS exposure, the adjusted positive association
375 was present at 6 months but stronger at 12 months of age; at 12 months we observed a Treg mean
376 value for above the median PFHXS of $0.45 \pm \text{SD: } 0.03$ (95%CI: 0.40, 0.50) versus a mean value for
377 below the median PFHXS of $0.32 \pm \text{SD: } 0.03$ (95%CI: 0.26, 0.38) (p-value for difference = 0.002);
378 similar trends for 12 months but not 6 months were observed for PFOS, PFOA, and PFNA (Figure
379 3D). No differences between the mean value of Th17 cells for above versus below median PFOS,
380 PFOA, PFNA, and PFHXS were observed (Figure 3E).

381 **Discussion**

382 In this prospective cohort study, we investigated the association between maternal PFAS exposure
383 CD4+ T-cell subpopulations in infants over the first year of life. The potential of PFAS to affect the
384 immune system has been widely reported in population studies across the world, with consistently
385 observed reductions in antibody responses to common childhood vaccinations.^{9,12} Yet, the specific
386 immune cell components altered by PFAS exposure remain unknown. We found that increased
387 concentrations of maternal PFAS were associated with a reduction in the percentage of Tfh cells,
388 increased Th2, Th1, and Treg populations, and no differences in Th17 cells. Moreover, each
389 association was stronger from birth to 12 months of age. These findings indicate that the potential
390 effects of prenatal PFAS exposure may become more pronounced as the infant grows older. This

391 could be attributed to ongoing T-cell development in the first year of life, and that certain T-cell
392 subpopulations may not emerge until the infant is exposed to specific stimuli. As time passes and
393 T-cell subpopulations continue to develop, the impact of PFAS exposure on the cells becomes
394 more apparent.

395 The immune system protects against pathogens through a coordinated network of cells, tissues,
396 and organs. CD4+ T-cells orchestrate the immune response, making it specific to the type of stimuli
397 received and aiding in the generation and maintenance of immune memory. Particularly, Tfh cells
398 help direct B-cells to produce long-lasting, high-affinity antibodies essential for immune memory.³⁵
399 This study revealed a negative association between the percentage of Tfh cells and maternal PFAS
400 exposure during pregnancy. A reduction in Tfh cells in infants is consistent with the observed
401 reductions in antibodies to childhood vaccinations.^{27,28,62-66} This provides potential mechanistic
402 insights into this observation because Tfh cells are essential for mature and durable antibody
403 responses.^{35,39,40,67}

404 Given the complexity of antibody responses, it is unlikely Tfh cells are the only immune cell type
405 altered by PFAS exposure. For example, we also observed that Tregs were enhanced with increased
406 maternal PFAS concentrations. Tregs are recognized for their immunosuppressive functions and
407 their capacity to inhibit the activation and proliferation of effector T-cells.^{68,69} Studies have
408 demonstrated that Tregs can reduce immune responses to vaccinations by suppressing effector
409 responses.^{70,71} An increase in Treg cells could suppress T-cell or B-cell responses, thereby
410 attenuating antibody production. More generally, an enrichment in Treg cells could support an
411 immunosuppressed environment, dampening the overall ability to fight infections. Therefore, an
412 increased proportion or function of Tregs could also contribute to reduced antibody titers that have
413 been observed in association with PFAS exposure.

414 In addition to Tfh and Tregs, our study found a positive association between the percent of Th1 and
415 Th2 cells with maternal PFAS concentrations. While Th1 and Th2 cells play important defense roles
416 during infections, excessive Th1 and Th2 activity can be involved in the immunopathogenesis of
417 several chronic health conditions, including allergy and autoimmunity.⁷²⁻⁷⁷ Th1 cells are among the
418 predominant T-cell subpopulations in systemic autoimmune disorders, such as rheumatoid
419 arthritis⁷⁸, as well as organ-specific autoimmunity, such as Type 1 diabetes mellitus⁷⁹, and other
420 debilitating inflammatory disorders such as Crohn's disease.⁸⁰

421 On the other hand, Th2 cells have been associated with the development of atopic and allergic
422 diseases such as atopic dermatitis, eczema, chronic rhinosinusitis, and asthma.^{77,81,82} While
423 studies have associated PFAS exposure with allergic or autoimmune outcomes in children, the
424 findings are inconsistent, with some showing no association.⁸³⁻⁹⁴ Several studies examining the
425 association between PFAS exposure and allergic outcomes in infants have measured IgE levels in
426 umbilical cord serum. For instance, Okada et al. in 2012⁸⁷ reported lower umbilical cord IgE levels
427 at birth associated with higher maternal PFOA, whereas Wang et al. in 2011⁸⁸ found increased IgE
428 levels in cord blood associated with prenatal PFOA and PFOS. IgE plays an important role in the
429 allergic response; however, baseline total IgE levels may not reliably predict allergic outcomes,
430 particularly because they are not specific to a particular allergen. Additionally, a study by Oulhole
431 et al. 2017⁹⁵ found a positive association between PFAS concentrations and basophil counts in 5-
432 year-old infants; while their study did not investigate allergic outcomes, it is well established that
433 basophils play a crucial role in initiating Th2-mediated immunity.⁹⁶ Thus, an enhancement in Th2
434 responses operates in concert with these innate immune cells, which could lead to the
435 development of adverse allergic outcomes. Type 2 cytokines such as IL-4, IL-5, and IL-13 have been
436 associated with asthma development, and Th2 cells are the primary source of these
437 cytokines.^{75,81,82} Similar to allergic outcomes, evidence for the association between PFAS exposure
438 and asthma has been mixed. Studies reporting negative associations between exposure to PFAS,
439 and the risk of asthma were mainly conducted in children under the age of 10,^{91,97} while those
440 reporting a positive association were conducted in adolescents.^{92,94,98} This emphasizes the
441 importance of considering age and longitudinal analysis when studying immune-related outcomes
442 in children.

443 Our findings reveal a 0.30 (95% CI: 0.18, 0.41) greater Th2 percentage associated with PFOA at 12
444 months. While the changes observed in the age-specific percentages of CD4+ T-cells in this study
445 may appear small, these variation sizes have had health implications in previous studies. For
446 instance, an estimated 1.5-2 fold increase in Th2 cells has been noted among infant patients with
447 atopic dermatitis or bronchial asthma compared to healthy controls.^{99,100} Using the mean Th2
448 percentage of 0.38% (\pm SD: 0.38) as a reference in our infants (Figure 1F, Supplemental Table 5), an
449 increase of 0.30 indicates an overall 79% increase in Th2 cells. Further, numerous studies have
450 shown that minor changes in the frequency of circulating T follicular helper (cTfh) cells correlate
451 with antigen-specific antibody levels in humans^{39,101-103}, at ranges similar to the 18% reduction in
452 Tfh cells we observed. Individuals with higher frequencies of cTfh cells typically exhibit more robust

453 antibody responses; this relationship has been observed in vaccine responses to hepatitis B¹⁰³,
454 yellow fever virus¹⁰², and influenza¹⁰¹, as well as among children infected with malaria³⁹.

455 Our findings provide strong evidence that maternal PFAS exposure affects the infant's immune
456 system. Differences in CD4+ T cell subpopulations as a function of maternal PFAS exposure
457 support the idea that PFAS are immunotoxic in human infants. As with all research studies using
458 human populations, this study has several strengths, as well as some limitations. One major
459 strength is that this is a longitudinal study with deep immunophenotyping, high-dimensional
460 analysis, and identification of infant CD4+ T-cell subpopulations. Additionally, since only healthy
461 pregnancies and full-term healthy infants were enrolled in the study, we partly removed the
462 potential for congenital-disease-related changes in CD4+ T-cell subpopulations that could
463 influence immunological outcomes. However, this study is not without limitations. The study
464 sample was relatively small (n=200) compared to larger cohort studies.^{26,27} However, even these
465 larger cohort studies that showed negative associations between PFAS and antibody titers did not
466 include in-depth immunophenotyping. These previous studies, therefore, leave a gap in our
467 understanding of the cells responsible for coordinating the antibody response. Moreover, although
468 it is well established that PFAS can cross the placenta^{20,104} and can be detected in the fetus²¹, in the
469 current study, PFAS were only measured during the second trimester of pregnancy and not directly
470 in the infants. Although this is a limitation, this exposure window is a crucial period for potential T-
471 cell programming and development.^{2,105} Human T-cell development begins around the 8th week of
472 pregnancy and continues after birth during infancy; exposures during T-cell development can
473 significantly affect the immune profile of the offspring.¹⁰⁶ For example, human cohort studies have
474 linked maternal exposure to pollutants and decreased T-cell-dependent immune defenses in
475 infants and children.^{28,107,108} Further evidence that developmental exposures shape T-cell function
476 is provided by experimental studies, which provide strong evidence that in-utero exposure can
477 significantly and durably alter T-cell function later in life.¹⁰⁹

478 Participants in the study had lower mean serum concentrations of PFOS, PFOA, and PFNA but
479 higher PFHXS compared to the general population levels reported by NHANES (2017-2018).⁶¹ The
480 current study provides insights for ongoing risk assessment of PFAS exposures since the legacy
481 PFAS levels are declining over time⁶¹ and our study suggests immunotoxic impacts in early life, even
482 at these lower levels.

483 Our results indicate stronger associations between maternal PFAS exposure and CD4+ T-cell
484 subpopulations later during infancy compared to birth. This is likely due to the fact that T-cells are
485 still developing at birth, and infants have not been exposed to the stimuli needed to activate and
486 differentiate T-cell subpopulations. Ongoing PFAS exposure after birth is a key factor to consider.
487 Recently, PFAS has been detected in human breast milk^{22,23} and could represent a continuous
488 source of maternally derived PFAS exposure in the early postnatal life. Rigorous studies to quantify
489 the variation of PFAS in breast milk and formula or other postnatal exposures and immune
490 development are warranted.

491 In conclusion, we report here an association between in utero exposure to PFAS and decreased
492 percent of Tfh cells and increased percent of Th1, Th2, and Treg cells during the first year of life.
493 These observations support that there are immunomodulatory effects of developmental PFAS
494 exposure. These findings contribute to our understanding of potential mechanisms by which PFAS
495 exposure lowers antibody titers in infants. Moreover, given that imbalances in T-cell subpopulations
496 are associated with other diseases, in-depth profiling of infant T-cells suggests that in utero PFAS
497 exposure may predispose to future immunopathogenesis.

498

499

500

501

502

503

504

505

506

507

508

509

510

511

512

513

514 **References**

- 515 1. Park JE, Botting RA, Domínguez Conde C, et al. A cell atlas of human thymic development
516 defines T cell repertoire formation. *Science*. 2020;367(6480):eaay3224.
517 doi:10.1126/science.aay3224
- 518 2. Zhang X, Zhivaki D, Lo-Man R. Unique aspects of the perinatal immune system. *Nat Rev*
519 *Immunol*. 2017;17(8):495-507. doi:10.1038/nri.2017.54
- 520 3. West LJ. Defining critical windows in the development of the human immune system. *Hum Exp*
521 *Toxicol*. 2002;21(9-10):499-505. doi:10.1191/0960327102ht288oa
- 522 4. Gómez-Roig MD, Pascal R, Cahuana MJ, et al. Environmental Exposure during Pregnancy:
523 Influence on Prenatal Development and Early Life: A Comprehensive Review. *Fetal Diagn Ther*.
524 2021;48(4):245-257. doi:10.1159/000514884
- 525 5. Prüss-Ustün A, Vickers C, Haefliger P, Bertollini R. Knowns and unknowns on burden of disease
526 due to chemicals: a systematic review. *Environ Health*. 2011;10(1):9. doi:10.1186/1476-069X-
527 10-9
- 528 6. Barouki R, Gluckman PD, Grandjean P, Hanson M, Heindel JJ. Developmental origins of non-
529 communicable disease: Implications for research and public health. *Environ Health*.
530 2012;11(1):42. doi:10.1186/1476-069X-11-42
- 531 7. Rychlik KA, Sillé FCM. Environmental exposures during pregnancy: Mechanistic effects on
532 immunity. *Birth Defects Research*. 2019;111(4):178-196. doi:10.1002/bdr2.1469
- 533 8. Buck RC, Franklin J, Berger U, et al. Perfluoroalkyl and polyfluoroalkyl substances in the
534 environment: Terminology, classification, and origins. *Integr Environ Assess Manag*.
535 2011;7(4):513-541. doi:10.1002/ieam.258
- 536 9. Antoniou E, Colnot T, Zeegers M, Dekant W. Immunomodulation and exposure to per- and
537 polyfluoroalkyl substances: an overview of the current evidence from animal and human
538 studies. *Arch Toxicol*. 2022;96(8):2261-2285. doi:10.1007/s00204-022-03303-4

- 539 10. Zhang X, Xue L, Deji Z, et al. Effects of exposure to per- and polyfluoroalkyl substances on
540 vaccine antibodies: A systematic review and meta-analysis based on epidemiological studies.
541 *Environmental Pollution*. 2022;306:119442. doi:10.1016/j.envpol.2022.119442
- 542 11. Blake BE, Fenton SE. Early life exposure to per- and polyfluoroalkyl substances (PFAS) and
543 latent health outcomes: A review including the placenta as a target tissue and possible driver of
544 peri- and postnatal effects. *Toxicology*. 2020;443:152565. doi:10.1016/j.tox.2020.152565
- 545 12. Zhang L, Louie A, Rigutto G, et al. A systematic evidence map of chronic inflammation and
546 immunosuppression related to per- and polyfluoroalkyl substance (PFAS) exposure. *Environ*
547 *Res*. 2023;220:115188. doi:10.1016/j.envres.2022.115188
- 548 13. Fenton SE, Ducatman A, Boobis A, et al. Per- and Polyfluoroalkyl Substance Toxicity and
549 Human Health Review: Current State of Knowledge and Strategies for Informing Future
550 Research. *Environ Toxicol Chem*. 2021;40(3):606-630. doi:10.1002/etc.4890
- 551 14. Birth Outcomes in Relation to Prenatal Exposure to Per- and Polyfluoroalkyl Substances and
552 Stress in the Environmental Influences on Child Health Outcomes (ECHO) Program.
553 doi:10.1289/EHP10723
- 554 15. Pérez F, Nadal M, Navarro-Ortega A, et al. Accumulation of perfluoroalkyl substances in human
555 tissues. *Environment International*. 2013;59:354-362. doi:10.1016/j.envint.2013.06.004
- 556 16. Lewis RC, Johns LE, Meeker JD. Serum Biomarkers of Exposure to Perfluoroalkyl Substances in
557 Relation to Serum Testosterone and Measures of Thyroid Function among Adults and
558 Adolescents from NHANES 2011–2012. *International Journal of Environmental Research and*
559 *Public Health*. 2015;12(6):6098. doi:10.3390/ijerph120606098
- 560 17. Cserbik D, Casas M, Flores C, et al. Concentrations of per- and polyfluoroalkyl substances
561 (PFAS) in paired tap water and blood samples during pregnancy. *J Expo Sci Environ Epidemiol*.
562 2024;34(1):90-96. doi:10.1038/s41370-023-00581-7
- 563 18. Göckener B, Weber T, Rüdell H, Bücking M, Kolossa-Gehring M. Human biomonitoring of per-
564 and polyfluoroalkyl substances in German blood plasma samples from 1982 to 2019.
565 *Environment International*. 2020;145:106123. doi:10.1016/j.envint.2020.106123

- 566 19. Duan Y, Sun H, Yao Y, Meng Y, Li Y. Distribution of novel and legacy per-/polyfluoroalkyl
567 substances in serum and its associations with two glycemic biomarkers among Chinese adult
568 men and women with normal blood glucose levels. *Environment International*.
569 2020;134:105295. doi:10.1016/j.envint.2019.105295
- 570 20. Ma D, Lu Y, Liang Y, et al. A Critical Review on Transplacental Transfer of Per- and Polyfluoroalkyl
571 Substances: Prenatal Exposure Levels, Characteristics, and Mechanisms. *Environ Sci Technol*.
572 2022;56(10):6014-6026. doi:10.1021/acs.est.1c01057
- 573 21. Mamsen LS, Björvang RD, Mucs D, et al. Concentrations of perfluoroalkyl substances (PFASs)
574 in human embryonic and fetal organs from first, second, and third trimester pregnancies.
575 *Environment International*. 2019;124:482-492. doi:10.1016/j.envint.2019.01.010
- 576 22. LaKind JS, Naiman J, Verner MA, Lévesque L, Fenton S. Per- and polyfluoroalkyl substances
577 (PFAS) in breast milk and infant formula: A global issue. *Environmental Research*.
578 2023;219:115042. doi:10.1016/j.envres.2022.115042
- 579 23. Zheng G, Schreder E, Dempsey JC, et al. Per- and Polyfluoroalkyl Substances (PFAS) in Breast
580 Milk: Concerning Trends for Current-Use PFAS. *Environ Sci Technol*. 2021;55(11):7510-7520.
581 doi:10.1021/acs.est.0c06978
- 582 24. Pan Y, Zhu Y, Zheng T, et al. Novel Chlorinated Polyfluorinated Ether Sulfonates and Legacy Per-
583 /Polyfluoroalkyl Substances: Placental Transfer and Relationship with Serum Albumin and
584 Glomerular Filtration Rate. *Environ Sci Technol*. 2017;51(1):634-644.
585 doi:10.1021/acs.est.6b04590
- 586 25. McAdam J, Bell EM. Determinants of maternal and neonatal PFAS concentrations: a review.
587 *Environmental Health*. 2023;22(1):41. doi:10.1186/s12940-023-00992-x
- 588 26. Grandjean P, Andersen EW, Budtz-Jørgensen E, et al. Serum Vaccine Antibody Concentrations
589 in Children Exposed to Perfluorinated Compounds. *JAMA*. 2012;307(4).
590 doi:10.1001/jama.2011.2034

- 591 27. Grandjean P, Heilmann C, Weihe P, Nielsen F, Mogensen UB, Budtz-Jørgensen E. Serum Vaccine
592 Antibody Concentrations in Adolescents Exposed to Perfluorinated Compounds. *Environ*
593 *Health Perspect.* 2017;125(7):077018. doi:10.1289/EHP275
- 594 28. Granum B, Haug LS, Namork E, et al. Pre-natal exposure to perfluoroalkyl substances may be
595 associated with altered vaccine antibody levels and immune-related health outcomes in early
596 childhood. *J Immunotoxicol.* 2013;10(4):373-379. doi:10.3109/1547691X.2012.755580
- 597 29. Kielsen K, Shamim Z, Ryder LP, et al. Antibody response to booster vaccination with tetanus
598 and diphtheria in adults exposed to perfluorinated alkylates. *Journal of Immunotoxicology.*
599 2016;13(2):270-273. doi:10.3109/1547691X.2015.1067259
- 600 30. Kaur K, Lesseur C, Chen L, et al. Cross-sectional associations of maternal PFAS exposure on
601 SARS-CoV-2 IgG antibody levels during pregnancy. *Environ Res.* 2023;219:115067.
602 doi:10.1016/j.envres.2022.115067
- 603 31. Nutt SL, Hodgkin PD, Tarlinton DM, Corcoran LM. The generation of antibody-secreting plasma
604 cells. *Nat Rev Immunol.* 2015;15(3):160-171. doi:10.1038/nri3795
- 605 32. Farber DL, Yudanin NA, Restifo NP. Human memory T cells: generation, compartmentalization
606 and homeostasis. *Nat Rev Immunol.* 2014;14(1):24-35. doi:10.1038/nri3567
- 607 33. Zhu J, Paul WE. Peripheral CD4+ T-cell differentiation regulated by networks of cytokines and
608 transcription factors: Transcription factor network in Th cells. *Immunological Reviews.*
609 2010;238(1):247-262. doi:10.1111/j.1600-065X.2010.00951.x
- 610 34. Parker DC. T cell-dependent B cell activation. *Annu Rev Immunol.* 1993;11:331-360.
611 doi:10.1146/annurev.iy.11.040193.001555
- 612 35. Song W, Craft J. T follicular helper cell heterogeneity: Time, space, and function. *Immunol Rev.*
613 2019;288(1):85-96. doi:10.1111/imr.12740
- 614 36. Crotty S. T follicular helper cell differentiation, function, and roles in disease. *Immunity.*
615 2014;41(4):529-542. doi:10.1016/j.immuni.2014.10.004

- 616 37. Ma CS, Deenick EK, Batten M, Tangye SG. The origins, function, and regulation of T follicular
617 helper cells. *J Exp Med*. 2012;209(7):1241-1253. doi:10.1084/jem.20120994
- 618 38. Suh WK. Life of T Follicular Helper Cells. *Mol Cells*. 2015;38(3):195-201.
619 doi:10.14348/molcells.2015.2331
- 620 39. Chan JA, Loughland JR, de la Parte L, et al. Age-dependent changes in circulating Tfh cells
621 influence development of functional malaria antibodies in children. *Nat Commun*.
622 2022;13(1):4159. doi:10.1038/s41467-022-31880-6
- 623 40. Sage PT, Alvarez D, Godec J, von Andrian UH, Sharpe AH. Circulating T follicular regulatory and
624 helper cells have memory-like properties. *J Clin Invest*. 2014;124(12):5191-5204.
625 doi:10.1172/JCI76861
- 626 41. Luckheeram RV, Zhou R, Verma AD, Xia B. CD4+T Cells: Differentiation and Functions. *Clin Dev*
627 *Immunol*. 2012;2012:925135. doi:10.1155/2012/925135
- 628 42. Alberts B, Johnson A, Lewis J, Raff M, Roberts K, Walter P. Helper T Cells and Lymphocyte
629 Activation. In: *Molecular Biology of the Cell. 4th Edition*. Garland Science; 2002. Accessed
630 September 24, 2024. <https://www.ncbi.nlm.nih.gov/books/NBK26827/>
- 631 43. Stavnezer J, Guikema JEJ, Schrader CE. Mechanism and Regulation of Class Switch
632 Recombination. *Annu Rev Immunol*. 2008;26:261-292.
633 doi:10.1146/annurev.immunol.26.021607.090248
- 634 44. Lu LL, Suscovich TJ, Fortune SM, Alter G. Beyond binding: antibody effector functions in
635 infectious diseases. *Nat Rev Immunol*. 2018;18(1):46-61. doi:10.1038/nri.2017.106
- 636 45. O'Connor T, Best M, Brunner J, et al. Cohort profile: Understanding Pregnancy Signals and
637 Infant Development (UPSIDE): a pregnancy cohort study on prenatal exposure mechanisms for
638 child health. *BMJ Open*. 2021;11(4):e044798. doi:10.1136/bmjopen-2020-044798
- 639 46. Knapp EA, Kress AM, Parker CB, et al. The Environmental Influences on Child Health Outcomes
640 (ECHO)-Wide Cohort. *American Journal of Epidemiology*. 2023;192(8):1249.
641 doi:10.1093/aje/kwad071

- 642 47. Honda M, Robinson M, Kannan K. A rapid method for the analysis of perfluorinated alkyl
643 substances in serum by hybrid solid-phase extraction. *Environ Chem*. 2018;15(2):92.
644 doi:10.1071/EN17192
- 645 48. Scheible K, Secor-Socha S, Wightman T, et al. Stability of T Cell Phenotype and Functional
646 Assays Following Heparinized Umbilical Cord Blood Collection. *Cytometry A*. 2012;81(11):937-
647 949. doi:10.1002/cyto.a.22203
- 648 49. McDavid A, Laniewski N, Grier A, et al. Aberrant newborn T cell and microbiota developmental
649 trajectories predict respiratory compromise during infancy. *iScience*. 2022;25(4):104007.
650 doi:10.1016/j.isci.2022.104007
- 651 50. Mei HE, Leipold MD, Maecker HT. Platinum-conjugated antibodies for application in mass
652 cytometry. *Cytometry Part A*. 2016;89(3):292-300. doi:10.1002/cyto.a.22778
- 653 51. Hartmann FJ, Simonds EF, Bendall SC. A Universal Live Cell Barcoding-Platform for Multiplexed
654 Human Single Cell Analysis. *Sci Rep*. 2018;8(1):10770. doi:10.1038/s41598-018-28791-2
- 655 52. Mei HE, Leipold MD, Schulz AR, Chester C, Maecker HT. Barcoding of live human peripheral
656 blood mononuclear cells for multiplexed mass cytometry. *J Immunol*. 2015;194(4):2022-2031.
657 doi:10.4049/jimmunol.1402661
- 658 53. Van Gassen S, Callebaut B, Van Helden MJ, et al. FlowSOM: Using self-organizing maps for
659 visualization and interpretation of cytometry data. *Cytometry Part A*. 2015;87(7):636-645.
660 doi:10.1002/cyto.a.22625
- 661 54. McInnes L, Healy J, Melville J. UMAP: Uniform Manifold Approximation and Projection for
662 Dimension Reduction. Published online September 18, 2020. Accessed November 5, 2024.
663 <http://arxiv.org/abs/1802.03426>
- 664 55. Bulka CM, Bommarito PA, Fry RC. Predictors of toxic metal exposures among US women of
665 reproductive age. *J Expo Sci Environ Epidemiol*. 2019;29(5):597-612. doi:10.1038/s41370-019-
666 0152-3

- 667 56. Rivera-Núñez Z, Kinkade CW, Khoury L, et al. Prenatal perfluoroalkyl substances exposure and
668 maternal sex steroid hormones across pregnancy. *Environ Res.* 2023;220:115233.
669 doi:10.1016/j.envres.2023.115233
- 670 57. Liston A, Humblet-Baron S, Duffy D, Goris A. Human immune diversity: from evolution to
671 modernity. *Nat Immunol.* 2021;22(12):1479-1489. doi:10.1038/s41590-021-01058-1
- 672 58. Kuznetsova A, Brockhoff PB, Christensen RHB. **lmerTest** Package: Tests in Linear Mixed Effects
673 Models. *J Stat Soft.* 2017;82(13). doi:10.18637/jss.v082.i13
- 674 59. Fox J, Weisberg S, Price B, et al. car: Companion to Applied Regression. Published online
675 September 27, 2024. Accessed November 14, 2024. [https://cran.r-](https://cran.r-project.org/web/packages/car/index.html)
676 [project.org/web/packages/car/index.html](https://cran.r-project.org/web/packages/car/index.html)
- 677 60. Posit team. RStudio: Integrated Development Environment for R. Posit. 2024. Accessed
678 November 5, 2024. <https://www.posit.co/>
- 679 61. CDC. Final Report: Findings Across Ten Exposure Assessment Sites. Per- and Polyfluoroalkyl
680 Substances (PFAS) and Your Health. November 7, 2024. Accessed November 12, 2024.
681 <https://www.atsdr.cdc.gov/pfas/final-report/index.html>
- 682 62. Timmermann CAG, Jensen KJ, Nielsen F, et al. Serum Perfluoroalkyl Substances, Vaccine
683 Responses, and Morbidity in a Cohort of Guinea-Bissau Children. *Environmental Health*
684 *Perspectives.* 2020;128(8):087002. doi:10.1289/EHP6517
- 685 63. Abraham K, Mielke H, Fromme H, et al. Internal exposure to perfluoroalkyl substances (PFASs)
686 and biological markers in 101 healthy 1-year-old children: associations between levels of
687 perfluorooctanoic acid (PFOA) and vaccine response. *Arch Toxicol.* 2020;94(6):2131-2147.
688 doi:10.1007/s00204-020-02715-4
- 689 64. Timmermann CAG, Pedersen HS, Weihe P, et al. Concentrations of tetanus and diphtheria
690 antibodies in vaccinated Greenlandic children aged 7–12 years exposed to marine pollutants, a
691 cross sectional study. *Environmental Research.* 2022;203:111712.
692 doi:10.1016/j.envres.2021.111712

- 693 65. Mogensen UB, Grandjean P, Heilmann C, Nielsen F, Weihe P, Budtz-Jørgensen E. Structural
694 equation modeling of immunotoxicity associated with exposure to perfluorinated alkylates.
695 *Environmental Health*. 2015;14(1):47. doi:10.1186/s12940-015-0032-9
- 696 66. Stein CR, McGovern KJ, Pajak AM, Maglione PJ, Wolff MS. Perfluoroalkyl and polyfluoroalkyl
697 substances and indicators of immune function in children aged 12–19 y: National Health and
698 Nutrition Examination Survey. *Pediatr Res*. 2016;79(2):348-357. doi:10.1038/pr.2015.213
- 699 67. Sage PT, Sharpe AH. T Follicular Regulatory Cells in the Regulation of B cell Responses. *Trends*
700 *Immunol*. 2015;36(7):410-418. doi:10.1016/j.it.2015.05.005
- 701 68. Wan YY. Regulatory T cells: immune suppression and beyond. *Cell Mol Immunol*.
702 2010;7(3):204-210. doi:10.1038/cmi.2010.20
- 703 69. Sojka DK, Huang YH, Fowell DJ. Mechanisms of regulatory T-cell suppression - a diverse arsenal
704 for a moving target. *Immunology*. 2008;124(1):13-22. doi:10.1111/j.1365-2567.2008.02813.x
- 705 70. Ndure J, Noho-Konteh F, Adetifa JU, et al. Negative Correlation between Circulating
706 CD4+FOXP3+CD127– Regulatory T Cells and Subsequent Antibody Responses to Infant
707 Measles Vaccine but Not Diphtheria–Tetanus–Pertussis Vaccine Implies a Regulatory Role.
708 *Front Immunol*. 2017;8. doi:10.3389/fimmu.2017.00921
- 709 71. Stepkowski S, Bekbolsynov D, Oenick J, et al. The Major Role of T Regulatory Cells in the
710 Efficiency of Vaccination in General and Immunocompromised Populations: A Review.
711 *Vaccines (Basel)*. 2024;12(9):992. doi:10.3390/vaccines12090992
- 712 72. Skapenko A, Leipe J, Lipsky PE, Schulze-Koops H. The role of the T cell in autoimmune
713 inflammation. *Arthritis Research & Therapy*. 2005;7(2):S4. doi:10.1186/ar1703
- 714 73. Romagnani S. Th1/Th2 cells. *Inflamm Bowel Dis*. 1999;5(4):285-294. doi:10.1097/00054725-
715 199911000-00009
- 716 74. Dardalhon V, Korn T, Kuchroo VK, Anderson AC. Role of Th1 and Th17 cells in organ-specific
717 autoimmunity. *J Autoimmun*. 2008;31(3):252-256. doi:10.1016/j.jaut.2008.04.017

- 718 75. Deo SS, Mistry KJ, Kakade AM, Niphadkar PV. Role played by Th2 type cytokines in IgE mediated
719 allergy and asthma. *Lung India*. 2010;27(2):66-71. doi:10.4103/0970-2113.63609
- 720 76. Bosnjak B, Stelzmueller B, Erb KJ, Epstein MM. Treatment of allergic asthma: Modulation of Th2
721 cells and their responses. *Respiratory Research*. 2011;12(1):114. doi:10.1186/1465-9921-12-
722 114
- 723 77. Brandt EB, Sivaprasad U. Th2 Cytokines and Atopic Dermatitis. *J Clin Cell Immunol*.
724 2011;2(3):110. doi:10.4172/2155-9899.1000110
- 725 78. Luo P, Wang P, Xu J, et al. Immunomodulatory role of T helper cells in rheumatoid arthritis: a
726 comprehensive research review. *Bone & Joint Research*. 2022;11(7):426. doi:10.1302/2046-
727 3758.117.BJR-2021-0594.R1
- 728 79. Walker LSK, Herrath M von. CD4 T cell differentiation in type 1 diabetes. *Clinical and*
729 *Experimental Immunology*. 2015;183(1):16. doi:10.1111/cei.12672
- 730 80. Imam T, Park S, Kaplan MH, Olson MR. Effector T Helper Cell Subsets in Inflammatory Bowel
731 Diseases. *Front Immunol*. 2018;9. doi:10.3389/fimmu.2018.01212
- 732 81. Harker JA, Lloyd CM. T helper 2 cells in asthma. *The Journal of Experimental Medicine*.
733 2023;220(6):e20221094. doi:10.1084/jem.20221094
- 734 82. León B. Understanding the development of Th2 cell-driven allergic airway disease in early life.
735 *Front Allergy*. 2023;3:1080153. doi:10.3389/falgy.2022.1080153
- 736 83. Rappazzo K, Coffman E, Hines E. Exposure to Perfluorinated Alkyl Substances and Health
737 Outcomes in Children: A Systematic Review of the Epidemiologic Literature. *IJERPH*.
738 2017;14(7):691. doi:10.3390/ijerph14070691
- 739 84. von Holst H, Nayak P, Dembek Z, et al. Perfluoroalkyl substances exposure and immunity,
740 allergic response, infection, and asthma in children: review of epidemiologic studies. *Heliyon*.
741 2021;7(10):e08160. doi:10.1016/j.heliyon.2021.e08160

- 742 85. Smit L a. M, Lenters V, Høyer BB, et al. Prenatal exposure to environmental chemical
743 contaminants and asthma and eczema in school-age children. *Allergy*. 2015;70(6):653-660.
744 doi:10.1111/all.12605
- 745 86. Okada E, Sasaki S, Kashino I, et al. Prenatal exposure to perfluoroalkyl acids and allergic
746 diseases in early childhood. *Environment International*. 2014;65:127-134.
747 doi:10.1016/j.envint.2014.01.007
- 748 87. Okada E, Sasaki S, Saijo Y, et al. Prenatal exposure to perfluorinated chemicals and relationship
749 with allergies and infectious diseases in infants. *Environmental Research*. 2012;112:118-125.
750 doi:10.1016/j.envres.2011.10.003
- 751 88. Wang IJ, Hsieh WS, Chen CY, et al. The effect of prenatal perfluorinated chemicals exposures
752 on pediatric atopy. *Environmental Research*. 2011;111(6):785-791.
753 doi:10.1016/j.envres.2011.04.006
- 754 89. Goudarzi H, Miyashita C, Okada E, et al. Effects of prenatal exposure to perfluoroalkyl acids on
755 prevalence of allergic diseases among 4-year-old children. *Environment International*.
756 2016;94:124-132. doi:10.1016/j.envint.2016.05.020
- 757 90. Wen HJ, Wang SL, Chuang YC, Chen PC, Guo YL. Prenatal perfluorooctanoic acid exposure is
758 associated with early onset atopic dermatitis in 5-year-old children. *Chemosphere*.
759 2019;231:25-31. doi:10.1016/j.chemosphere.2019.05.100
- 760 91. Jackson-Browne MS, Eliot M, Patti M, Spanier AJ, Braun JM. PFAS (per- and polyfluoroalkyl
761 substances) and asthma in young children: NHANES 2013–2014. *International Journal of*
762 *Hygiene and Environmental Health*. 2020;229:113565. doi:10.1016/j.ijheh.2020.113565
- 763 92. Humblet O, Diaz-Ramirez LG, Balmes JR, Pinney SM, Hiatt RA. Perfluoroalkyl Chemicals and
764 Asthma among Children 12–19 Years of Age: NHANES (1999–2008). *Environmental Health*
765 *Perspectives*. 2014;122(10):1129-1133. doi:10.1289/ehp.1306606
- 766 93. Zhu Y, Qin XD, Zeng XW, et al. Associations of serum perfluoroalkyl acid levels with T-helper
767 cell-specific cytokines in children: By gender and asthma status. *Science of The Total*
768 *Environment*. 2016;559:166-173. doi:10.1016/j.scitotenv.2016.03.187

- 769 94. Dong GH, Tung KY, Tsai CH, et al. Serum Polyfluoroalkyl Concentrations, Asthma Outcomes,
770 and Immunological Markers in a Case–Control Study of Taiwanese Children. *Environmental*
771 *Health Perspectives*. 2013;121(4):507-513. doi:10.1289/ehp.1205351
- 772 95. Oulhote Y, Shamim Z, Kielsen K, et al. Children’s white blood cell counts in relation to
773 developmental exposures to methylmercury and persistent organic pollutants. *Reproductive*
774 *Toxicology*. 2017;68:207-214. doi:10.1016/j.reprotox.2016.08.001
- 775 96. Nakanishi K. Basophils are potent antigen-presenting cells that selectively induce Th2 cells.
776 *European Journal of Immunology*. 2010;40(7):1836-1842. doi:10.1002/eji.201040588
- 777 97. Beck IH, Timmermann CAG, Nielsen F, et al. Association between prenatal exposure to
778 perfluoroalkyl substances and asthma in 5-year-old children in the Odense Child Cohort.
779 *Environmental Health: A Global Access Science Source*. 2019;18(1). doi:10.1186/s12940-019-
780 0541-z
- 781 98. Kvaalem HE, Nygaard UC, Lødrup Carlsen KC, Carlsen KH, Haug LS, Granum B. Perfluoroalkyl
782 substances, airways infections, allergy and asthma related health outcomes – implications of
783 gender, exposure period and study design. *Environment International*. 2020;134:105259.
784 doi:10.1016/j.envint.2019.105259
- 785 99. Kawamoto N, Kaneko H, Takemura M, et al. Age-related changes in intracellular cytokine
786 profiles and Th2 dominance in allergic children. *Pediatric Allergy and Immunology*.
787 2006;17(2):125-133. doi:10.1111/j.1399-3038.2005.00363.x
- 788 100. Brunner PM. Early immunologic changes during the onset of atopic dermatitis. *Annals of*
789 *Allergy, Asthma & Immunology*. 2019;123(2):152-157. doi:10.1016/j.anai.2019.03.033
- 790 101. Herati RS, Reuter MA, Dolfi DV, et al. Circulating CXCR5+PD-1+ Response Predicts Influenza
791 Vaccine Antibody Responses in Young Adults but not Elderly Adults. *The Journal of*
792 *Immunology*. 2014;193(7):3528-3537. doi:10.4049/jimmunol.1302503
- 793 102. Huber JE, Ahlfeld J, Scheck MK, et al. Dynamic changes in circulating T follicular helper cell
794 composition predict neutralising antibody responses after yellow fever vaccination. *Clinical &*
795 *Translational Immunology*. 2020;9(5):e1129. doi:10.1002/cti2.1129

- 796 103. Yin M, Xiong Y, Liang D, et al. Circulating Tfh cell and subsets distribution are associated
797 with low-responsiveness to hepatitis B vaccination. *Molecular Medicine*. 2021;27(1):32.
798 doi:10.1186/s10020-021-00290-7
- 799 104. Verner MA, Ngueta G, Jensen ET, et al. A Simple Pharmacokinetic Model of Prenatal and
800 Postnatal Exposure to Perfluoroalkyl Substances (PFASs). *Environ Sci Technol*. 2016;50(2):978-
801 986. doi:10.1021/acs.est.5b04399
- 802 105. Park JE, Jardine L, Gottgens B, Teichmann SA, Haniffa M. Prenatal development of human
803 immunity. *Science*. 2020;368(6491):600-603. doi:10.1126/science.aaz9330
- 804 106. Netea MG, Domínguez-Andrés J, Barreiro LB, et al. Defining trained immunity and its role in
805 health and disease. *Nat Rev Immunol*. 2020;20(6):375-388. doi:10.1038/s41577-020-0285-6
- 806 107. Hochstenbach K, van Leeuwen DM, Gmuender H, et al. Toxicogenomic profiles in relation to
807 maternal immunotoxic exposure and immune functionality in newborns. *Toxicol Sci*.
808 2012;129(2):315-324. doi:10.1093/toxsci/kfs214
- 809 108. Stølevik SB, Nygaard UC, Namork E, et al. Prenatal exposure to polychlorinated biphenyls
810 and dioxins from the maternal diet may be associated with immunosuppressive effects that
811 persist into early childhood. *Food and Chemical Toxicology*. 2013;51:165-172.
812 doi:10.1016/j.fct.2012.09.027
- 813 109. Boule LA, Winans B, Lawrence BP. Effects of developmental activation of the AhR on CD4+
814 T-cell responses to influenza virus infection in adult mice. *Environ Health Perspect*.
815 2014;122(11):1201-1208. doi:10.1289/ehp.1408110
- 816
817
818
819
820
821
822
823

824 **Table 1:** Infant and maternal characteristics. (n=200)

Characteristic	Mean ± SD
Gestational Age (weeks)	39.74 ± 1.11
Birth Weight (grams)	3411.39 ± 464.49
Maternal Age	N (%)
18-25	41(20.5)
26-35	142(71)
36+	17(8.5)
Pre-pregnancy BMI	
Underweight	1(0.5)
Normal Weight	90(45)
Overweight	50(25)
Obese	59(29.5)
Annual Income	
Lower Class	41(20.5)
Lower-Middle Class	48(24)
Middle Class	40(20)
Upper-Middle Class	34(17)
Upper Class	19(9.5)
Not Reported	18(9)
Parity	
0	69(34.5)
1	78(39)
2+	53(26.5)
Infant Sex	
Male	105(52.5)
Female	95(47.5)
Mode of Delivery	
Vaginal	153(76.5)
Caesarian	47(23.5)
Maternal Race	
White	125(62.5)
Asian	40(20)
Black	16(8)
Hispanic	9(4.5)
Other	10(5)
Maternal Education	
HS or Less	64(32)
Some college	31(15.5)
Bachelors	54(27)

Postgraduate	50(25)
Not Reported	1(0.5)
<hr/>	
Medicaid During Pregnancy	
No	114(57)
Yes	86(43)

825 BMI: Body Mass Index, SD: Standard deviation, HS: High School

826

827

828

829

830

831

832

833

834

835

836

837

838

839

840

841

842

843

844

845

846

847

848

849

850

851

852

853 **Table 2:** Distribution of perfluoroalkyl substances (PFAS) in maternal plasma (ng/mL).

PFAS	Mean	SD	Min	1 st Q	Median	3 rd Q	Max
PFOS	2.87	2.13	0.61	1.83	2.51	3.22	21.30
PFOA	0.68	0.51	0.06	0.40	0.59	0.83	5.45
PFNA	0.33	0.36	0.06	0.17	0.24	0.35	2.87
PFHXS	1.96	0.92	0.56	1.38	1.75	2.42	7.17

854 PFOS: perfluorooctanesulfonic acid, PFOA: perfluorooctanoic acid, PFHxS: perfluorohexane
855 sulfonic acid, PFNA: perfluorononanoic acid, PFDA: perfluorodecanoic acid, SD: Standard
856 Deviation, Min: minimum, Max: Maximum, LOD: limit of detection, Q: quantile.

857

858

859

860

861

862

863

864

865

866

867

868

869

870

871

872

873

874 **Main Text Figure Captions**

875 **Figure 1:** *Identification of CD4+ T-cell subpopulations in infants and their age-associated*
876 *frequencies.*

877 (A) Study design and T-cell analysis pipeline. (B) Uniform Manifold Approximation and Projection
878 (UMAP) representation of FlowSOM nodes colored by major peripheral blood mononuclear
879 cells (PBMC): CD4+, CD8+, CD14+, CD19+, CD56+, TCR $\gamma\delta$; (C) Stacked bar graph denoting the
880 proportion of CD45RA+ and CD45RO+ CD4+ T-cell subpopulations at birth, 6 and 12 months of age.
881 (D-E) UMAP representation of FlowSOM nodes colored by expression of (D) CD45 isoform type
882 (CD45RA+ or CD45RO+) within CD4+ T-cell FlowSOM nodes, and (E) CD4+ T-cell sub-cluster
883 annotations based on the following marker expression: Treg (FOXP3+CD127-), Th1(IFN γ +), Th17 (IL-
884 17A+), Tfh (IL-21+), Th2 (IL-4+), Naïve-cytokine-negative (TN). Circle size on UMAPs represents the
885 relative mean count of total cells assigned to each FlowSOM node. (F) Frequency of CD4+ T-cells in
886 cord blood at birth and PBMC at six and twelve months. Each dot on the boxplots denotes data
887 from an individual infant at the indicated age; scales for boxplots are fixed.

888

889 **Figure 2:** *Maternal PFAS exposure associates with infant CD4+ T-cell frequencies in an age-*
890 *dependent manner.*

891 The plots illustrate the regression lines for the age-specific average marginal effects of the
892 association between continuous maternal PFAS (ng/mL) exposure and infant CD4+ T-cell
893 percentage. Rows represent individual CD4+ T-cells: (A) T follicular helper cells, (B) T helper 2 cells,
894 (C) T helper 1 cells, (D) T regulatory cells, and (E) T helper 17 cells. Columns represent individual
895 PFAS; PFOS, PFOA, PFNA, and PFHXS were log₂ transformed. The colors represent the infant age:
896 birth (grey), 6 months (orange), and 12 months (blue). Each dot represents an individual infant at
897 the indicated age. Age-specific average marginal effects (β) were adjusted for the categorical
898 covariates parity, infant sex, and continuous pre-pregnancy body mass index. Parenthesis next to
899 each age-specific β contains the 95% confidence interval for the estimate. Pairwise comparisons
900 between the age-specific β s are represented by the brackets. Asterisks denote statistically
901 significant (p -value < 0.05), and 'ns' indicates non-statistically significant differences between age-
902 specific β s. Axis are independent for each CD4+ T-cell subpopulation and each PFAS.
903 Supplemental Tables 6, 7, and 8 contain corresponding numeric data.

904

905 **Figure 3:** *Maternal PFAS exposure predicts CD4+ T-cell trajectories in infants.*

906 The plots illustrate differences-over-time between infant CD4+ T-cell subpopulations by a
907 categorical PFAS value (below versus above median value). Rows represent individual CD4+ T-cells:
908 (A) T follicular helper cells, (B) T helper 2 cells, (C) T helper 1 cells, (D) T regulatory cells, and (E) T
909 helper 17 cells. Columns represent individual PFAS (PFOS, PFOA, PFNA, and PFHXS). The colors
910 represent the categorical PFAS value: below the median (pink) and above the median (blue). Dots
911 denote the predicted marginal mean of each CD4+ T-cell subpopulation at the indicated age.
912 Marginal means were adjusted for the categorical covariates parity, infant sex, and continuous pre-
913 pregnancy body mass index. Error bars represent the standard error of the marginal means. P-
914 values denote the statistical significance between marginal means contrasting below vs. above the
915 median PFAS; the contrast was considered statistically significant if the p-value < 0.05. The y-axis is
916 independent for each CD4+ T-cell subpopulation. Supplemental Tables 9, 10, and 11 contain
917 corresponding numeric data.

918

919

920

921

922

923

924

925

926

927

928

929

930

931

932

933

934

935

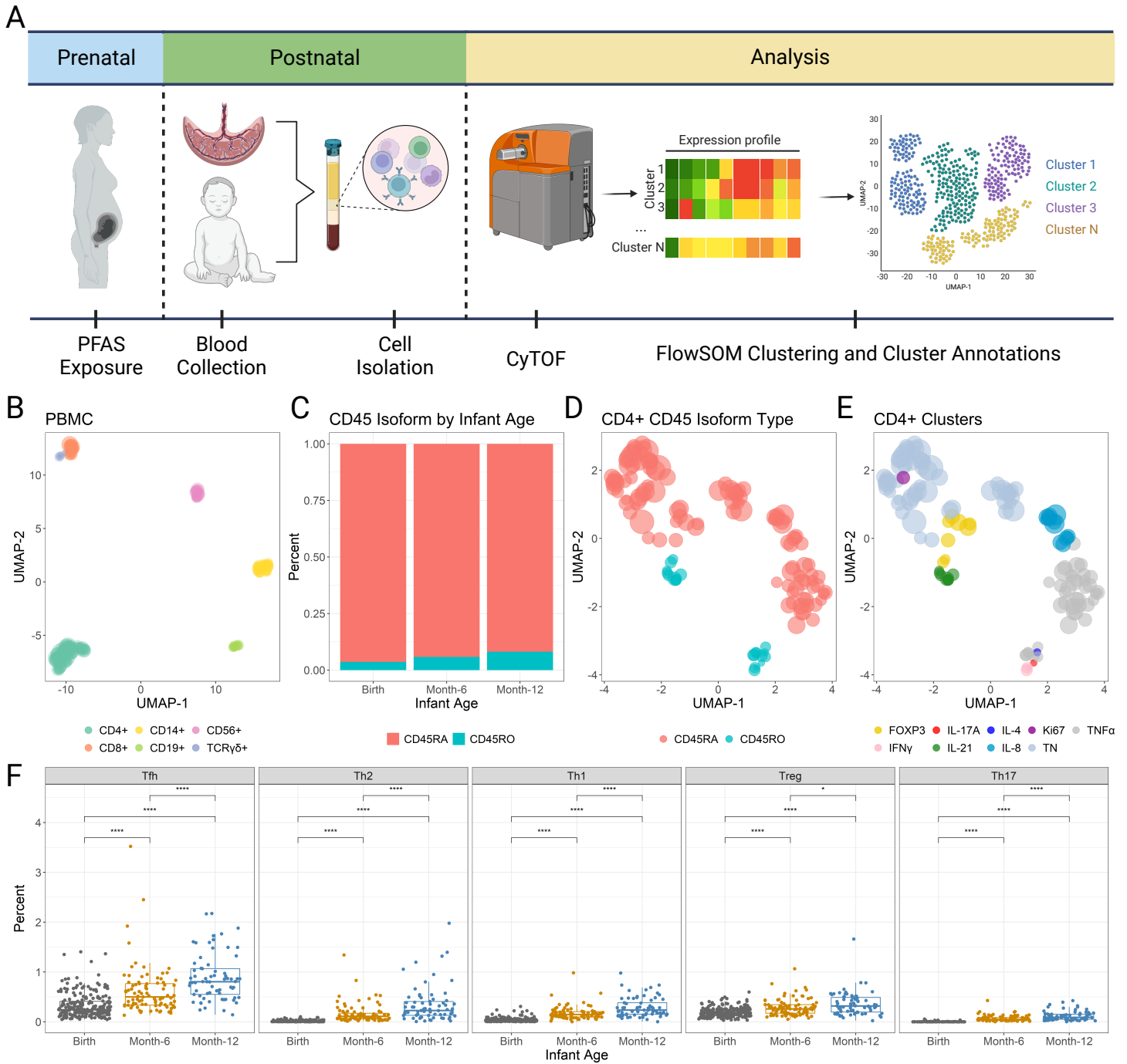
936

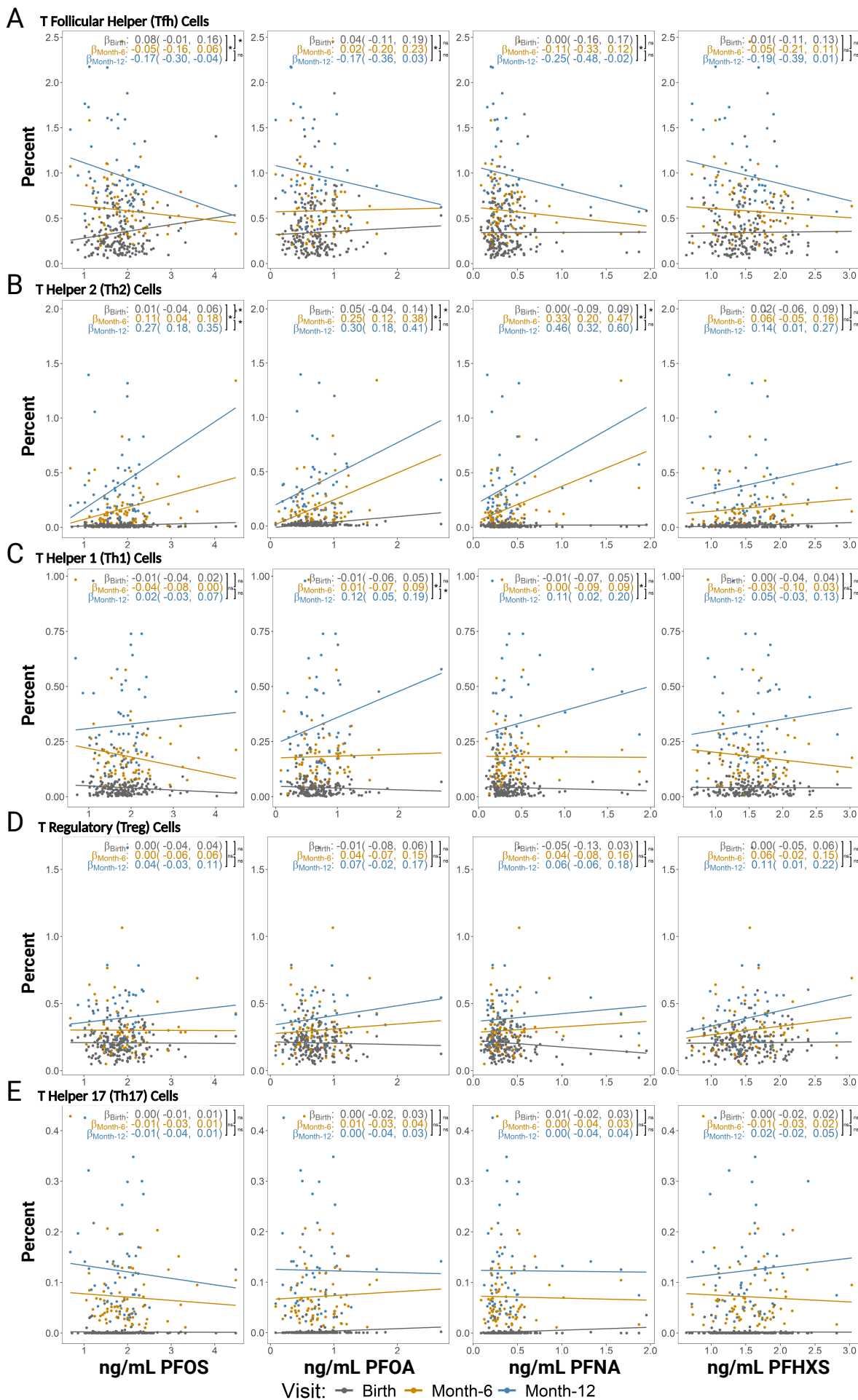
937

938 **Acknowledgments:**

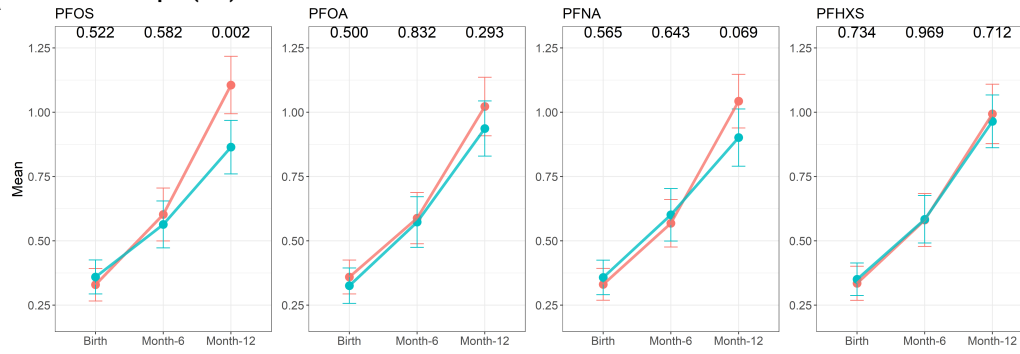
939 Authors would like to acknowledge the support of the mothers and infants participating in UPSIDE-
940 ECHO, UPSIDE-ECHO staff, University of Rochester Flow Cytometry Core, Scheible lab members
941 Adam Geber, Janiret Narvaez Miranda, Dean for their technical assistance. Research reported in
942 this publication was supported by the funding sources: NIH (OD) UH3OD023349, NIH (OD)
943 UG3OD02349, NIH (NIAID) T32AI007285, NIH (NIEHS) P30ES001247, NIH (NIEHS) R01ES036197,
944 NIH (NICHD) R01HD083369, NIH (NCATS) University of Rochester Clinical and Translational
945 Science Award UL1TR002001. The Wynne Center for Family Research. The content is solely the
946 responsibility of the authors and does not necessarily represent the official views of the National
947 Institutes of Health.

948

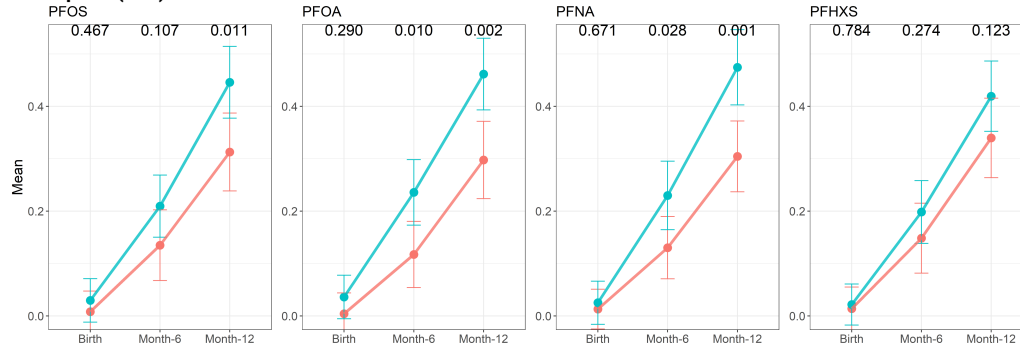




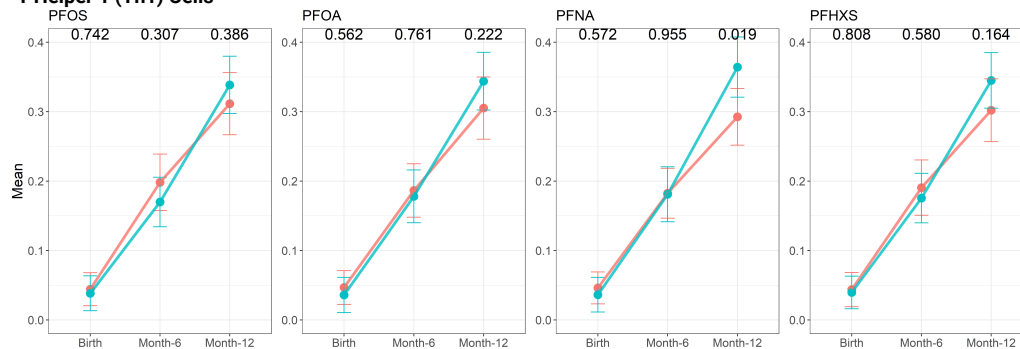
A T Follicular Helper (Tfh) Cells



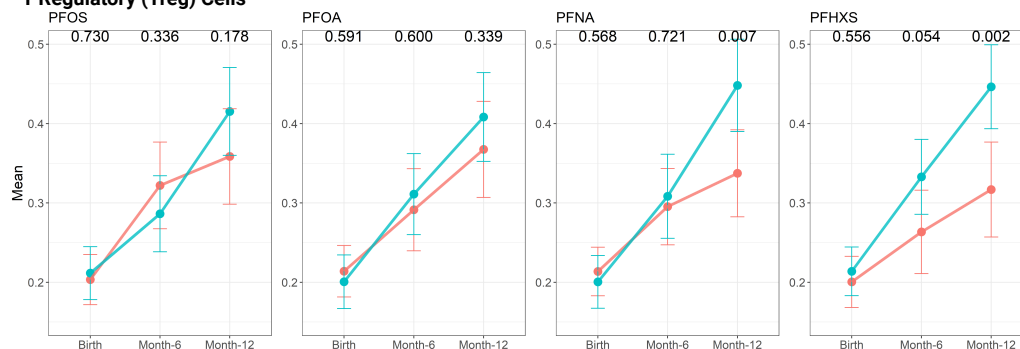
B T Helper 2 (Th2) Cells



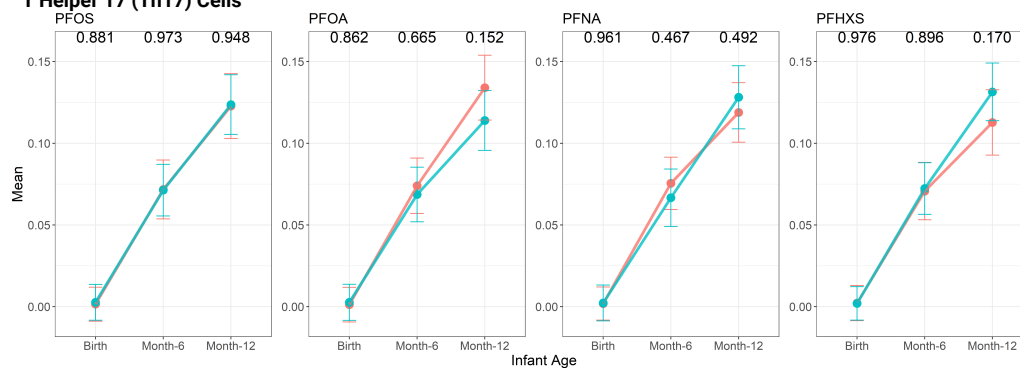
C T Helper 1 (Th1) Cells



D T Regulatory (Treg) Cells



E T Helper 17 (Th17) Cells



PFAS ● Below-Median ● Above-Median